

# OPTIMUM SEMI-CODELESS CARRIER PHASE TRACKING OF L2

K. T. Woo

*NavCom Technology, Inc., Redondo Beach, California*

## BIOGRAPHIES

Dr. K. T. Woo received his BS, MS, and Ph.D. degrees in Electrical Engineering from the University of California, Los Angeles in 1964, 1966, and 1970 respectively. He is one of the co-founders of NavCom Technology, Inc., which has recently become an affiliated company of Deere and Company. Previously, Dr. Woo was with the Aerospace Corporation in El Segundo, California. His areas of interest include GPS, DGPS and WAAS receivers and DGPS networks, spread spectrum communications, as well as signal processing and interference mitigation techniques. He has received three U.S. patents in the areas of GPS receiver design and application.

## ABSTRACT

GPS satellites transmit spread spectrum signals on L1 and L2 at 1575.42 and 1227.6 MHz, respectively. The Coarse/Acquisition (C/A) code and the precision (P) code modulate the L1 signal. The L2 signal is modulated by the P-code only. GPS receivers measure the carrier and code phases of the L1 and L2 signals from a number of GPS satellites to compute the position of the receiver and the time at which the measurements are collected. To prevent spoofing of the military P-code signals, an encrypted code, called the W code, which is not available to civilian users, is modulated by the Department of Defense with the publicly known P code on both L1 and L2 to provide the anti-spoofing Y-code. Since L2, unlike L1, does not have the C/A code, its access is denied to all users without knowledge of the W-code. This has severe impacts on survey, carrier phase differential, and kinematic users who need rapid carrier phase ambiguity resolution that requires the difference frequency between L1 and L2 (the so-called Widelane Frequency). The widelane frequency has a wavelength that is 4.5 times larger than L1.

Without knowledge of the Y-code, one has to apply a codeless or a semi-codeless technique for the

reconstruction of the L2 carrier phase. Most receivers utilize a hybrid technique. The L1 carrier is recovered after C/A code correlation, and the L2 carrier is reconstructed without knowledge of the Y or W codes. There are four known techniques that have been published in the past: squaring, cross-correlation, P-code aided L2 squaring, and Z-tracking. Because of the lack of knowledge of the W code, these techniques perform significantly worse (14 to 31 dB at a typical L2  $C/N_0$ ) than an ideal phase lock loop.

This paper presents five additional techniques that can be used to reconstruct the L2 carrier without knowledge of the W-code. These five techniques are: 1) Code-aided L2 Costas loop with W-Bit integrate and dump arm filtering; 2) P-code aided L1, L2 Cross Correlation; 3) Soft decision Z-tracking; 4) Optimum L2 demodulation motivated by maximum a posteriori (MAP) estimation theory; and 5) Linear approximation of the MAP approach. The first three techniques are modification of existing techniques, with improved performance. Techniques 4 and 5 are optimum and near optimum techniques based on statistical estimation theory. A detailed derivation of the MAP approach is given. Also presented is a detailed comparison of the squaring losses of the various L2 recovery techniques as functions of received L2  $C/N_0$ 's. The performance of the MAP technique and its linear approximation is shown to be at least 3 dB better than all techniques published previously. In addition, it is analytically shown that the MAP approach provides the minimum squaring loss that is possible, and represents an upper bound of achievable performance for L2 carrier recovery without knowledge of the W-code. Computer simulation results agree with theory.

## INTRODUCTION

This paper discusses the performance of various codeless and semi-codeless techniques that can be used to obtain the carrier-phase measurement of the L2 suppressed carrier signal without knowledge of the encrypted anti-

spoofing (AS) Y-code. An approach that is motivated by Maximum A Posteriori (MAP) estimation theory is shown to be the theoretical optimum approach in terms of squaring loss, and will thus provide the best performance in terms of cycle slips. The advantage of having a L2 carrier phase measurement in addition to L1 is discussed in some detail in this Introduction.

A GPS receiver collects measurements from a number of orbiting satellites. These measurements are used to compute the position of the receiver and the time at which the measurements were received. For many applications, the required accuracy is much more than what is available to the Standard Positioning Service (SPS) users which is limited to 100 m horizontal and 156 m vertical with a probability of 95%. To provide decimeter to centimeter level of accuracy the receiver computes its position relative to another receiver, which is also collecting GPS measurements. The relative position can generally be determined much more accurately than the absolute position because error sources common to both receivers are cancelled in the computation.

Each GPS satellite transmits two spread-spectrum signals, on L1 (1575.42 MHz) and L2 (1227.6 MHz). Two signals are employed so that the refraction of the signals as they pass through the ionosphere can be measured and removed. C/A (Coarse/Acquisition) and the P (Precision) codes modulate the L1 carrier. Only the P-code modulates L2.

Because the C/A code can be used to make range measurements almost as good as the P code, the Department of Defense has implemented a process called selective availability (S/A) which is intended to deny civilian and unauthorized users the full accuracy of the system. When S/A is turned on, the satellite carrier frequency and pseudorandom modulation codes are caused to vary in an unpredictable manner such that a timing or range error is introduced into the code measurements. In addition, orbital information is modified so that the receiver cannot determine the satellite position as accurately. The combination of these two effects causes the measured pseudorange to contain a larger error than would otherwise be present; and the capability of the receiver to determine an accurate position is reduced.

In addition to the S/A capability, the Department of Defense has also implemented a process called anti-spoof (A/S), which is intended to prevent a terrorist or enemy from generating a signal which looks like a GPS satellite that could be used to "spoo" or fool a GPS receiver into computing a false position. When A/S is turned on, an additional pseudorandom code, generally referred to as the W code, is modulo-2 added on top of the P code. While the P code is publicly known, the W code is not.

The combination of the W code with the P code is usually referred to as the Y code. From measurements taken with high gain dish antennas, it has been determined that the W code "chip" rate is at approximately 500 KHz or 1/20th the "chip" rate of the P code. The W-Bit timing relationship relative to the P-code can also be determined this way.

Since the L2 signal is not modulated by the C/A code, a standard receiver would, when A/S is turned on, have no access to the Y code and, hence, no access to the L2 frequency. This loss of access to the L2 signal presents distinct problems to some user groups. First, it means that there is no means to measure and correct for the ionospheric refraction effects on the pseudorange measurements. This is not a problem to most users since the S/A itself has already induced positioning errors larger than that caused by the ionospheric refraction. However, it can be a problem to some of those who have implemented differential techniques for limiting the effects of S/A. The lack of access to the L2 frequency affects the survey user and the carrier-phase differential, or "kinematic" user, as well as the code-differential user who applies refraction corrected dual frequency carrier phase smoothing of code to improve accuracy.

Kinematic or carrier-phase differential techniques are a natural outcome of the use of GPS for surveying applications [1]. Rather than making use of the code measurements, which are adversely affected by multipath reflections, the reconstructed carrier-phase measurements are used in surveying and kinematic applications. The higher accuracy, which can be obtained from the carrier-phase measurements, is related to the relative wavelengths involved. The wavelength of the L1 carrier is 19 cm, and the wavelength of the L2 carrier 24.4 cm. A common rule of thumb is that a measurement can be made to a precision that is about 1/50th of the wavelength. Thus, a carrier-phase measurement can be obtained which is much more accurate than the code measurements. However, the carrier-phase measurement has one very significant disadvantage compared to the code measurements. Specifically, carrier-phase measurements can be used to derive an accurate range only if the correct number of whole cycles of carrier in transit between the satellite and the receiver can be determined in some manner. An equivalent requirement for use in a differential application is to determine the difference in the number of whole cycles at the reference receiver and the kinematic receiver. Unlike code measurements, carrier phase measurements are ambiguous because the receiver is not able to directly measure the whole number of cycles in the user to satellite range at the time of signal acquisition.

Several methods of determining the cycle ambiguity have

been developed [2-10]. In the first method used in surveying applications two or more static receivers collect carrier phase data to a common set of satellites for one to several hours. The baseline reduction process makes use of the change in satellite geometry to resolve the integer carrier phase ambiguities and baseline vector components. Once the whole-cycle ambiguity values are set the position can be recomputed; and, typically, this revised solution results in differential positions good to less than one centimeter.

Recently, other more sophisticated methods have been developed and used to resolve the whole-cycle ambiguities in the carrier-phase measurements for the moving or "kinematic" receiver. Like the survey applications, they depend upon a static reference receiver that is used to measure the systematic errors in the code and carrier measurements and transmit them in real time to the kinematic receiver. Typically, these ambiguity-resolution methods make use of both the code and carrier measurements in a multistep process. First, the code measurements are used to obtain a differential position whose accuracy is on the order of 1 to 5 meters. Next, an uncertainty region or volume of space is defined around the code differential position that has a high probability of containing the true solution. Finally, combinations of whole-cycle ambiguity values are chosen for each carrier-phase measurement such that the resultant carrier-phase solution both (1) lies within the uncertainty volume and (2) has a small RMS residual. At least five satellites are required because at least one redundant measurement is needed in order to compute residuals. The motion of the satellites ensures that the residuals will grow on any solution that is not correct. Only the one true solution should continue to yield small RMS residuals as the satellite moves.

The ability to measure full-cycle L1 and L2 carrier phase and dual frequency code pseudoranges (four-observables) provides a wealth of information that can be exploited. Wide-lane (86 cm wavelength) and ionosphere-free observables are examples of useful carrier phase combinations when L1 and L2 carrier phases are available.

There is a significant advantage with the use of longer carrier wavelengths. First, the number of combinations of whole-cycle ambiguities which will have solutions within any given uncertainty volume decreases as the cube of the wavelength involved. Second, the closer a false solution is to the true position the greater the amount of satellite motion required to cause the residuals of that solution to grow an equal amount. Both of these factors favor the use of the L2 carrier over the L1 carrier since the L2 wavelength is almost 30 percent longer than the L1 wavelength. However, the major motivation to obtain L2 carrier-phase measurements arises for another reason.

Specifically, the difference measurements obtained by subtracting the L2 carrier-phase measurements from the L1 measurements have a wavelength of 86 centimeters, which corresponds to the wavelength of the difference frequency of L1 minus L2. This wavelength is 4.5 times longer than the L1 wavelength and means that there will be approximately  $(4.5)^3$  or about 100 fewer combinations of whole-cycle ambiguities whose position will lie within the same uncertainty volume. Furthermore, the required satellite motion needed to cause the RMS residuals to exceed the elimination threshold will be at least 4.5 times smaller. In summary, there is a very large benefit to the whole-cycle ambiguity resolution process when carrier-phase measurements can be obtained on the L2 carrier.

### EXISTING L2 CARRIER PHASE TECHNIQUES WITHOUT KNOWLEDGE OF THE Y-CODE

The large benefit from L2 carrier-phase measurements has resulted in the development of several methods for obtaining the required measurements even in the event that A/S is turned on and normal access to the L2 signal is denied. Most of the receivers provide a hybrid technique. The L1 carrier is reconstructed by code-correlation using the C/A code, and a codeless or semi-codeless technique is applied to construct the L2 carrier. In the codeless technique no knowledge of the Y-code is assumed. In the semi-codeless technique the receiver assumes the knowledge of the publicly known Pcode which has a bandwidth (chip rate) of 10.23 MHz, and the fact that the Y-code is a modulo-2 sum of the P-code and an encrypted, unknown W-code, which has a bandwidth of approximately 500 KHz. Four different methods found in the literature are described below.

#### Squaring

This method (see [2], [11]) is to square the L2 signal, that is, to multiply it by itself, to remove the biphasic Y-code modulation and result in a unmodulated, continuous wave output, whose phase can be measured. A block diagram of this approach is given in Figure 1.

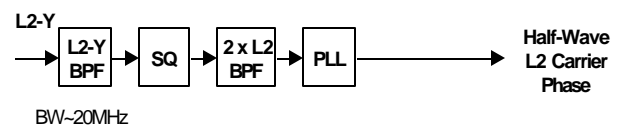


Figure 1. L2 Squaring ([2], [11])

The received L2 signal is bandpass filtered by an L2-Y bandpass filter, which has a bandwidth of approximately 20 MHz, or wide enough to pass the Ycode spread spectrum signal. The filter output is squared. The squared signal is filtered by another bandpass filter centered at the 2 x L2 frequency. A phase-lock-loop tracking the 2 x L2

frequency is used to reconstruct the phase of the  $2 \times L2$  carrier.

There are two significant disadvantages of the squaring process. First, the output frequency is twice the original carrier frequency and, hence, the wavelength is cut in half, resulting in a half-wavelength ambiguity. For survey and kinematic applications, this has all the disadvantages of shorter wavelengths described earlier. The second, even more serious, disadvantage is that the squaring process must be performed in a bandwidth broad enough to include most of the spread-spectrum energy of the incoming signal. Because this bandwidth also includes significantly more noise energy, the signal-to-noise ratio in the loop bandwidth is degraded by 30 dB (this is commonly referred to as the squaring loss, and is  $C/N_0$  dependent) as compared to a direct correlation process of recovering the carrier frequency.

### Cross-Correlation

A second method, developed in [12], overcomes the first of the two disadvantages described above. By multiplying the incoming L2 signal, not by itself, but instead by the incoming L1 signal in a process generally referred to as cross-correlation, the original L2 carrier-frequency signal is recovered. Thus, the wavelength is not cut in half as it is in the squaring process. Figure 2 is a block diagram of this technique.

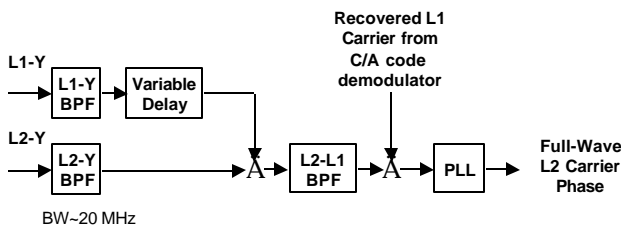


Figure 2. L1 x L2 Cross-Correlation [12]

When the L1 and L2 signals are transmitted from the satellite, the P code modulation of the two signals is synchronized. However, the ionospheric refraction causes a greater delay in the L2 signal than in the L1 signal. Thus, in order to maximize the signal strength, the L1 signal must be delayed by a variable amount in order to align the P code modulation of the two signals. The delayed L1-Y signal is multiplied with the L2-Y signal to remove the Y-code modulation, resulting in a continuous wave L1-L2 frequency. The phase of the L1-L2 (wide-lane) frequency can be used for integer ambiguity resolution. Alternatively, as shown in figure 2, the output of the bandpass filter, centered at the L1-L2 difference frequency, can be mixed with a reconstructed L1 carrier from C/A code correlation. The mixer output contains a L2 component that is tracked by a phase-lock-loop to recover the L2 carrier phase. The cross-correlation (i.e.,

multiplying the delayed L1-Y signal with the L2-Y signal) must still be done in the wide bandwidth of the spread-spectrum signals; consequently the large loss in signal-to-noise ratio seen in the squaring method remains. A recovery of 3 dB in squaring loss relative to the squaring process is obtained because the transmitted energy in the L1 signal is 3 dB greater than the energy in the L2 signal.

### P-code Aided L2 Squaring

A third method, known as P code aided squaring, for recovering the L2 carrier phase in the presence of A/S, is given in [13]. Figure 3 illustrates this technique.

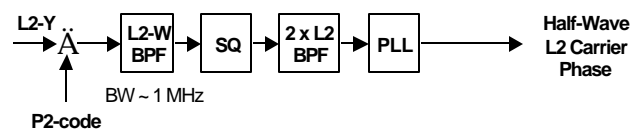


Figure 3. P-code Aided Squaring [13]

Because the Y code is a composite of both P code and W code modulation, it is possible to remove the P code component of the modulation using a locally generated replica of the P code (designated as P2 code in figure 3, for the L2 Pcode). Assuming that the P code can be successfully removed, only the W code modulation will remain. While the energy in the incoming L2 signal is spread over  $\pm 10$  MHz, after the removal of the P code modulation the W code modulation causes the energy to be spread over only  $\pm 500$  kHz. This allows the signal to be squared in a bandwidth that is 20 times narrower than was used in the original squaring method. This narrower bandwidth reduces the noise energy by 13 dB as compared to the original squaring process. Thus, instead of the original 30 dB squaring loss only 17db squaring loss is suffered. A significant disadvantage of this method is the doubling of the carrier frequency that results from the squaring process. Thus, the wavelength of the L2 phase measurement is half that obtained using the cross-correlation method.

### Z-Tracking

The cross-correlation technique improved the original squaring process by eliminating the doubling of the carrier frequency. The Pcode aided squaring technique improved the original squaring process by reducing the pre-squaring bandwidth, and achieves a substantially lower squaring loss. Z-Tracking [14] takes the next step that combines the cross-correlation technique with the reduced bandwidth obtained from P code aiding, as well as taking advantage of the timing relationship of the W-bits relative to the P-code. The particular method used to achieve the result was to make use of the approximate 20 to 1 ratio of the W code bit duration as compared to the P

code chip duration. Each of the L1 and L2 input signals is processed in such a way as to obtain estimates of the W code on a bit-by-bit basis. Figure 4 illustrates the basic concept of Z-Tracking for L2 carrier phase recovery without knowledge of the W-code data polarities.

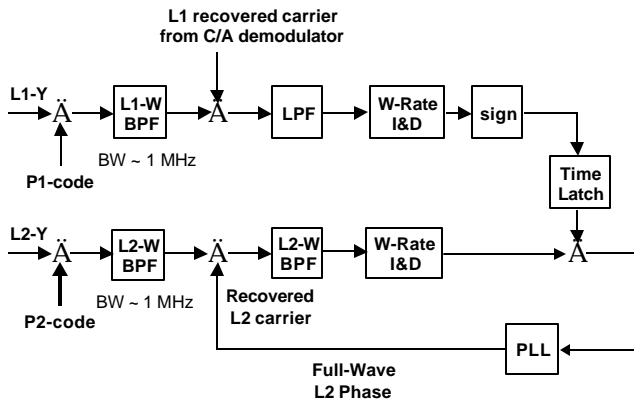


Figure 4. Z-Tracking for L2 Phase Recovery [14]

As illustrated in figure 4, both L1-Y and L2-Y signals are correlated with local P-codes of the L1 and L2 channels. Assume the local P-code is aligned with the received P-code, which can be achieved by maximizing the envelope of the correlator outputs. Then the L1-Y and L2-Y signals, after P-code correlation, have on them only the W-bit modulation with a bandwidth of approximately 1 MHz. In the L1 channel, the L1-W BPF output is demodulated with a local L1 carrier, which is recovered from correlation with the C/A code. The baseband output of the LPF is detected by a W-rate integrate-and-dump (I&D) filter, whose timing is derived from the P1 code and the timing relationship between P-code and W-bits observed with a high gain antenna. The sign of the integrate-and-dump output is an estimate of the W-code bit on L1. A similar process is applied to the L2-Y signal. Because the L2 signal is delayed by ionospheric refraction more than the L1 signal, the L2 P-code is a delayed version of the L1 P-code. Thus a single P-code generator with a variable delay can serve the same function as the two P-code generators depicted in figure 4. This was the implementation of ZTracking described in [14]. The L2-Y signal after correlation with a local L2 P-code is demodulated with an estimate of the L2 carrier, from a VCO (or NCO, in a digital implementation) in the L2 phase-lock-loop. The LPF output in the L2 path is again integrate-and-dump filtered, according to L2 P-code timing. The L2 integrate-and-dump output is cross-correlated with the time-latched value of the sign of the corresponding L1-W-bit estimate obtained from the L1 path. If timing alignment is maintained, the W-bit modulation on the L2 integrate-and-dump output is removed by the sign of the L1 W-bit in this process,

leaving a full-wave L2 carrier signal to be tracked by the phase-lock-loop. Thus Z-tracking provides a significant improvement over the P-code aided L2 squaring approach in that full-wavelength L2 carrier phase is obtained. The W-bit intervals need not be known precisely, but from independent determinations it is approximately equal to 20 chips of the P code. Because the L1 signal has 3 dB more power than the L2 signal, and because the P code bandwidth has been reduced to the bandwidth of the W code by cross correlation of the P Code replica prior to the detection of the individual W bits, the squaring loss will be less than P-code aided squaring, and substantially less than that of the original squaring method. However, while the Z-Tracking method described in [14] allows the recovery of the full wavelength of the L2 carrier and has a lower squaring loss than any of the other methods described earlier, it is still suboptimum in that it estimates the individual W code bits by a hard decision, i.e., each bit is determined to be one of two binary values, i.e. a one or a minus one. The Z-Tracking technique performs approximately 3 dB better than P-code aided L2 squaring. Thus, the squaring loss is approximately 13-14 dB. In the next section, the squaring loss of the various loop structures described above will be analyzed in more detail.

## SQUARING LOSS OF EXISTING TECHNIQUES

Squaring loss is generally used to designate the loss in signal-to-noise in the bandwidth of a phase-lock-loop used to recover the carrier of a suppressed-carrier signal, as compared to an ideal phase-lock-loop that is used to track a continuous-wave (CW) sinusoid without data modulation. Costas loop, squaring loop, as well as the  $n^{\text{th}}$  power loop are examples of phase-lock-loops of this type. Many authors have studied the squaring loss of various suppressed carrier recovery loops and their false-lock behaviors (e.g., see [15], [16], [17], and [18]). These earlier results can be used to characterize the squaring loss of the various existing L2 carrier recovery techniques described in the previous sections, as well as their modifications to be described in the next section. In brief, the squaring loss of a squaring loop, or a Costas loop, is related to the RMS phase error of the loop by the following equation

$$\mathbf{S}_f^2 = \left[ \frac{C}{N_o B_L} S_L \right]^{-1} \quad (1)$$

In (1)  $\mathbf{S}_f$  is the RMS phase error of the loop,  $C/N_o$  is the received carrier to noise power spectral density ratio,  $B_L$  is the loop bandwidth, and  $S_L$  is the squaring loss factor. Equation (1) is only a linear approximation of the loop behavior. But it is an accurate approximation for nominal loop design conditions when the RMS phase error is

small. For an ideal phase lock loop tracking a CW signal, the squaring loss factor  $S_L$  is unity, i.e., there is no squaring loss. In a suppressed carrier signal tracking loop a nonlinear operation is generally used to wipe-off the data (or code) modulation in order to create a CW signal for the phase-lock-loop to track. Noise product terms are generated in this nonlinear process, which degrade the signal to noise ratio in the loop bandwidth, and result in squaring loss. It is well known that the squaring loss of a Costas loop is identical to that of a squaring loop (see, e.g., [15]). For a Costas loop with arm filters having a transfer function  $H(f)$ , or, for a squaring loop with a pre-squaring BPF with the same low-pass equivalent transfer function, the squaring loss of a Costas or squaring loop with arbitrary arm (or pre-squaring) filter characteristics is given in [18]:

$$S_L = \frac{\left( \int_{-\infty}^{\infty} |H(f)|^2 S_m(f) df \right)^2}{\int_{-\infty}^{\infty} |H(f)|^4 S_m(f) df + \frac{1}{2(C/N_o)} \int_{-\infty}^{\infty} |H(f)|^4 df} \quad (2)$$

In (2)  $H(f)$  is the transfer function of the low-pass equivalent of the pre-squaring BPF (or, the arm filter of the Costas loop), and  $S_m(f)$  is the power spectrum of the bi-phase data (or code) modulation having polarities  $\pm 1$ . Assume the pre-squaring BPF is wide enough so that there is no signal distortion, then the squaring loss given in (2) for a general squaring loop can be approximated by

$$S_L \cong \frac{1}{1 + \frac{N_o B_P}{2C}} \quad (3)$$

In (3)  $B_P$  is used to designate the RF bandwidth of the BPF preceding the squarer in the squaring loop, and  $C/N_o$  is the L2 received carrier to noise power spectral density ratio. The squaring loss of both the squaring, cross-correlation, and P-code aided L2 squaring techniques can be computed with equation (3), with variations in  $B_P$  and  $C/N_o$ , as follows. In the squaring technique,  $B_P$  is approximately 20 MHz, since the BPF preceding the squarer has to be wide enough to pass the 10 M-chips/second Ycode. In the cross-correlation approach,  $B_P$  is again 20 MHz. However, since L1-Y is used to cross-correlate with L2-Y, and since L1-Y is 3 dB higher in power than L2-Y, the effective  $C/N_o$  going into the phase-lock-loop is twice that of L2. In the P-code aided L2 squaring approach, the  $C/N_o$  used in (3) is the same as that used in computing  $S_L$  of the squaring approach, and equals to the L2  $C/N_o$ . However, since the squaring operation is performed after Pcode correlation, the RF

bandwidth  $B_P$  of the pre-squaring BPF in the P-code aided squaring technique is only 1 MHz approximately.

The squaring loss of a Costas loop with data bit-rate integrate and dump arm filters and a hard-limited inphase-channel is also well known (see [15]). It is given by the following:

$$S_L = \text{erf}^2 \sqrt{CT / N_o} \quad (4)$$

In (4)  $\text{erf}(x)$  is the error-function,  $T$  is the bit-interval of the integrate-and-dump arm filters, and  $C/N_o$  is the carrier-to-noise density ratio seen by the loop. Equation (4) can be used to compute the squaring loss of the Z-Tracking approach, with the following modifications. First, the bit time is now the W-bit interval  $T_W$ , since the L1-Y and L2-Y signals are integrate-and-dump filtered at the W-bit rate after P-code correlation. Second, the  $C/N_o$  seen by the loop is actually twice that of the L2  $C/N_o$ , since the sign estimate of the L1 W-bit is used to multiply the L2 integrate-and-dump output, and since L1 is 3 dB higher in power than L2. Thus the squaring loss of Z-tracking is given by

$$S_L = \text{erf}^2 \sqrt{2CT_W / N_o} \quad (5)$$

where  $T_W$  designates the W-bit interval, which is approximately equal to 2 microseconds, and  $C/N_o$  is the L2 received carrier to noise density ratio.

Figure 5 plots the squaring loss of the four existing approaches. At the L2  $C/N_o$  of 39 dB-Hz, the squaring losses are -31, -28, -18, and -14 dB respectively for squaring, cross-correlation, P-code aided L2 squaring, and Z-Tracking.

## MODIFICATIONS OF EXISTING TECHNIQUES

From the discussions given in the previous two sections we observe that performance improvement in L2 codeless and semi-codeless techniques evolves over time, and is developed by modifying earlier approaches in order to reduce squaring loss and to achieve full wavelength L2 carrier recovery. For example, cross-correlation is an improvement over squaring since it gives a full-wavelength carrier phase and is 3 dB less in squaring loss. Similarly, Pcode aided L2 squaring is a modification of the original squaring approach, with a significant squaring loss reduction. And Z-Tracking is a further modification of both the cross-correlation and P-code aided squaring approaches, which results in full-wavelength carrier recovery and a further reduction in squaring loss. It is thus

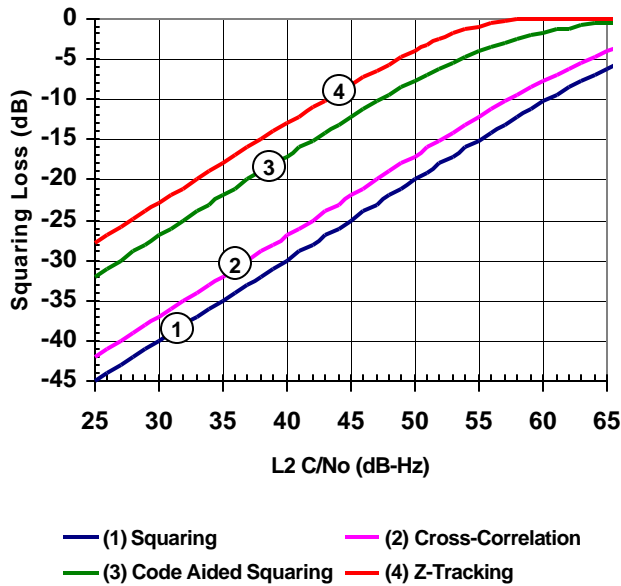


Figure 5. Squaring Loss of Existing Techniques

of interest to investigate if further modification can be made, with regard to squaring loss reduction in particular. Squaring loss increases the RMS phase error in the loop, which in turn can significantly increase the cycle slip probability. Cycle slips can cause data loss and are very undesirable in a static or kinematic survey operation. Thus it is desirable to minimize squaring loss as much as possible.

In this section we give three modifications of the previously discussed techniques. They can be shown to provide further performance improvements in terms of squaring loss. In a later section a MAP motivated approach and its linear approximation will also be presented, and shown to provide the optimum performance. The approaches presented here were disclosed earlier in an U.S. patent [19].

### P-Code Aided Cross Correlation

This method of recovering L2 phase measurements when the W code is enabled has not been discussed in open literature previously. It can be described as a method that simultaneously achieves the full wavelength advantage of the cross-correlation method and the improved signal-to-noise ratio advantage of the Pcode aided L2 squaring technique. It is a straightforward combination of the two methods. The principle of operation of this method is illustrated in figure 6.

In this method, the incoming L1 and L2 signals are each correlated with a locally generated P code signal. By first correlating with the P code, the bandwidth of the cross-

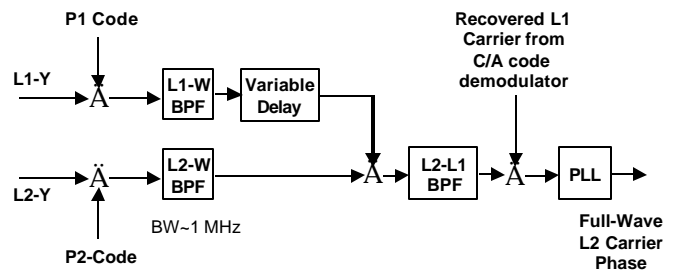
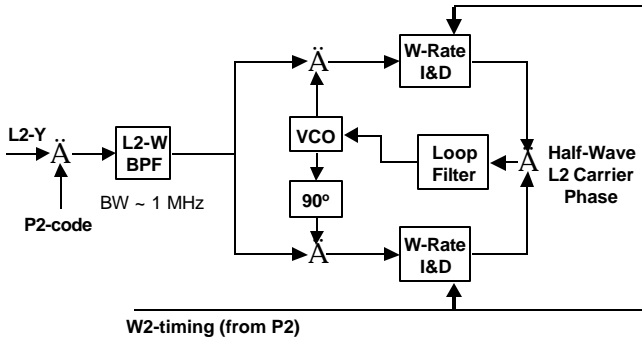


Figure 6. P-code Aided Cross-Correlation

correlated process can be reduced from 20 MHz to 1 MHz. The L1 signal is delayed to counteract the differential delay of the ionosphere and to match the phase of the W code in the two signal streams. The L1 and L2 signals are then cross-correlated to recover the full wavelength L2 carrier phase. The signal strength is maximized by adjusting the time delay to bring the two W codes into phase agreement. This method retains all the advantages of the cross-correlation and P-code aided L2 squaring methods in a single mechanism. Specifically, the signal-to-noise ratio is better than the cross-correlation method and full wavelength carrier phase measurements are available on the L2 channel, unlike the P-code aided squaring method. It is also significant that this new implementation gives a signal-to-noise ratio within one dB of the Z-Tracking method in a potentially simpler receiver design.

### P-Code Aided L2 Costas with WRate Integrate and Dump (I&D) Arm Filters

The next method described here represents an improvement of the Pcode aided L2 squaring method, and has also not been described in open literature previously. Like the Pcode aided L2 squaring method the processing involves only the L2 signal path and results in half wavelength cycle ambiguities in the L2 carrier phase measurements. The advantage of the new method is an improvement of 3 dB in squaring loss. The code wipe-off process is implemented in this method by a Costas loop structure with quadrature integrate-and-dump arm filters over the W-bit time interval. The principle of operation of this method is illustrated in figure 7. The L2 signal is first correlated with the locally generated P code and bandpass filtered to the 1 MHz bandwidth of the W code. Quadrature (sine and cosine) components of the phase error are generated with the local VCO. These components are integrated over one W-bit interval, and multiplied against each other to wipe-off the W-code modulation. The product of the quadrature sine and cosine channels gives an error term equal to the sine of twice the L2 phase error term. This means that the Costas loop can lock up either in phase or 180 degrees out of phase with respect to the incoming L2 carrier phase.



**Figure 7. P-code Aided L2 Costas with W-Rate Integrate-and-Dump Arm Filters**

The result out of the VCO is a full wavelength L2 carrier phase, but it is ambiguous at the half wavelength value. However, because this approach takes advantage of the W-bit timing, the integrate-and-dump arm filters are matched filters for the W-code modulation. As a result, this method has a 3-dB advantage over the P-code aided squaring technique in squaring loss.

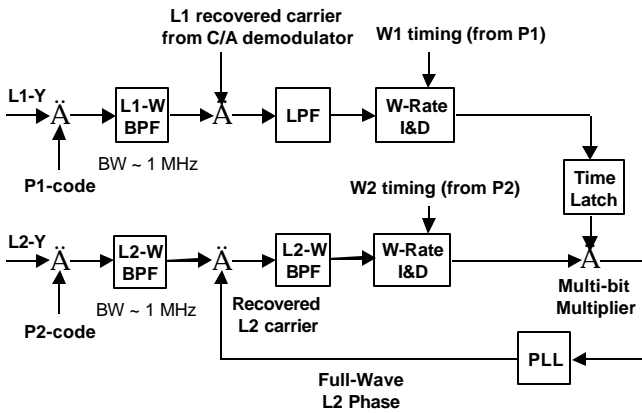


**Figure 8. Soft Decision Z-Tracking**

### Soft Decision Z-Tracking

In the ZTracking technique described in figure 4 the value of the W-bit is determined to be either a +1 or a -1 with a "hard decision". The soft-decision Z-Tracking method is a modification of the Z-Tracking technique in that a "soft decision" process is used instead of hard decision. The advantage of soft-decision over hard decision (~ 2dB) is well known in Viterbi decoding [20]. In the soft decision process used in this method, the actual value obtained from the W-Rate integrate-and-dump filter output in the L1 path is used rather than its sign only. The multiplier which forms the product of the L1 and L2 W-Rate integrate-and-dump filter outputs is now a multi-bit,

four-quadrant multiplier instead of the chopper multiplier that was used to perform this function in figure 4. Similar to Viterbi decoding, the use of soft decision improves the squaring loss of this approach by ~ 2 dB as compared to hard decision Z-Tracking. Figure 8 illustrates this method.

The squaring losses of these three modifications of existing techniques can be computed as follows. The squaring loss for the P-code aided cross correlation approach is formally the same as that of the cross-correlation technique discussed earlier, except that the bandpass filter bandwidth preceding the cross-correlation multiplier is now ~ 1 MHz instead of 20 MHz, i.e.,

$$S_L \cong \frac{1}{1 + \frac{N_o B_W}{4C}} \quad (6)$$

where  $B_W$  is ~ 1 MHz and is the two-sided bandwidth of the W-code spectrum, and  $C/N_o$  is the L2 received carrier to noise density ratio. The factor 4 arrives from cross-correlation, and the fact that L1 is 3 dB higher in power than L2.

The squaring loss for P-code aided L2 Costas with I&D Arm Filters can be computed with the known result given for conventional (i.e., not with a hard-limited I-channel) Costas loop with I&D arm filters as follows [15]:

$$S_L \cong \frac{1}{1 + \frac{1}{2CT_w / N_o}} \quad (7)$$

In (7)  $T_w$  is the W-bit time, which is approximately 2 microseconds, and  $CT_w/N_o$  is the L2 signal-to-noise ratio in the W-bit rate bandwidth, i.e., the L2 energy per W-Bit over noise power spectral density ratio.

The squaring loss for soft-decision Z-Tracking can also be computed with the above formulae, except there is a 3 dB increase in W-bit energy to noise density ratio, which arrives again from cross-correlation and the difference in power between L1 and L2. This squaring loss is given by:

$$S_L \cong \frac{1}{1 + \frac{1}{4CT_w / N_o}} \quad (8)$$

Figure 9 compares the squaring losses of the above three modifications of existing techniques. At the L2  $C/N_o$  of 39 dB-Hz the squaring loss of the Pcode aided cross-correlation approach is -15 dB, which is significantly better than the original cross-correlation approach (-28 dB). The squaring loss of the P-code aided L2 Costas with W-bit I&D arm filters is also -15 dB at 39 dB-Hz, and is 3



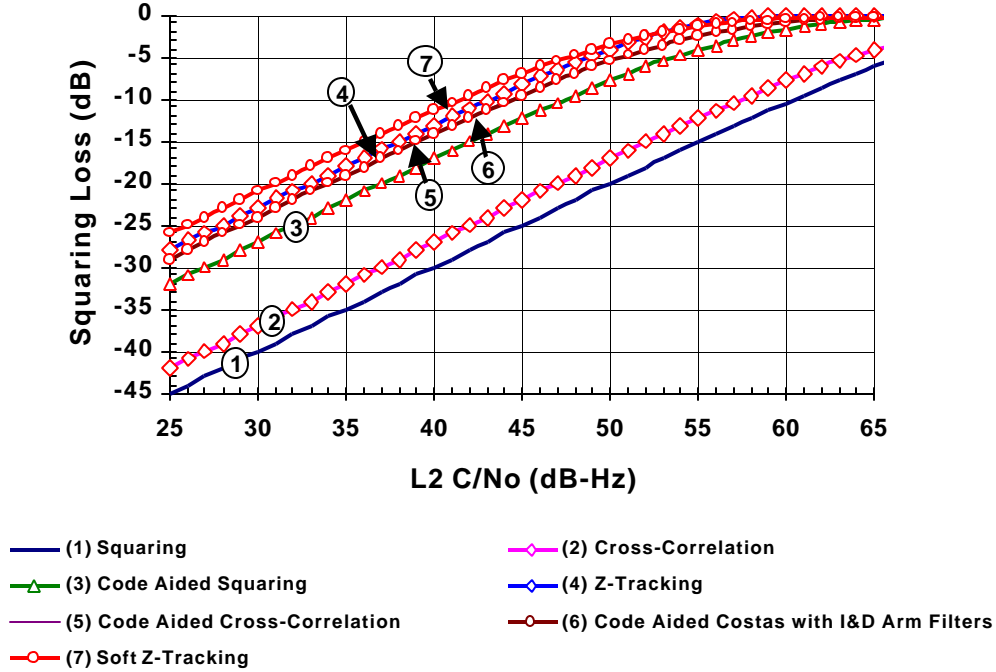


Figure 9. Squaring Losses of Modification of Existing Techniques

dB better than the original P-code aid L2 squaring approach (-18 dB). Since the Pcode aided L2 Costas approach provides only half wavelength carrier phase recovery, it is not as desirable as the P-code aided cross-correlation approach as they both have the same squaring loss. However, this did not consider hardware implementation.

The squaring loss of the soft-decision Z-Tracking approach is -12 dB at 39 dB-Hz, and is 2 dB better than the original Z-Tracking approach (-14 dB).

#### OPTIMUM DEMODULATION OF L2 MOTIVATED BY MAXIMUM A POSTERIORI (MAP) ESTIMATION THEORY

In this section we apply MAP estimation theory to derive an optimal demodulator for the L2 carrier phase when the W-bit data is random, i.e., unknown. From the gradient equation, which gives the solution of the MAP estimate of the L2 phase, a MAP motivated closed loop structure can be developed. And we can also prove that this structure is the optimum loop structure for L2 carrier recovery without knowledge of the encrypted Y-code. The following gives a derivation of the MAP estimator.

After the received L1 and L2 signals are correlated with the local P-code estimates and demodulated with the local L1 and L2 carriers we have the following three observables:

$$\begin{aligned} Q_1(t) &= r_1(t)p(t)\sqrt{2}\cos(\mathbf{w}_1t)|_{LP} = \sqrt{2S}d_k\cos\mathbf{q}_1 + n_{1s}(t) \\ Q_2(t) &= r_2(t)p(t)\sqrt{2}\cos(\mathbf{w}_2t)|_{LP} = \sqrt{S}d_k\cos\mathbf{q}_2 + n_{2s}(t) \quad (9) \\ I_2(t) &= -r_2(t)p(t)\sqrt{2}\sin(\mathbf{w}_2t)|_{LP} = \sqrt{S}d_k\sin\mathbf{q}_2 + n_{2c}(t) \end{aligned}$$

where

$Q_1(t)$  is the quadrature baseband signal after L1 is correlated with the local L1 P-code and carrier;

$Q_2(t)$  is the quadrature baseband signal after L2 is correlated with the local L2 P-code and carrier;

$I_2(t)$  is the inphase baseband signal after L2 is correlated with the local L2 P-code and carrier;

$r_1, r_2$  = the received L1 and L2 signals;

$n_{1c}, n_{2c}, n_{2s}$  = independent zero mean white Gaussian noise processes with (two-sided) noise power spectral density  $N_o/2$ ;

$\mathbf{w}_1, \mathbf{w}_2$  = radian frequencies of nominal L1 and L2;

$\mathbf{q}_1, \mathbf{q}_2$  = phases of L1 and L2;

$d_k = +/- 1$  random W-bit data;

S = L2 signal power;

2S=L1 signal power;

P(t)=Local L1 and L2 P-code estimates;

and LP denotes the low-pass components of the composite signal. Since L1 is in phase lock by tracking on the C/A channel, there is no phase error on L1. And without loss of generality, we can assume  $\theta_1=0$ . It is also assumed that L1 is 3 dB higher in power than L2.

The conditional joint Gaussian probability density function of the observed samples of  $Q_1, Q_2$  and  $I_2$  over one W-bit duration, given the L2 phase  $\theta_2$  and the W-bit data polarity, is given by:

$$P(Q_1, Q_2, I_2 | \mathbf{q}_2, d_k) = A \exp \left\{ \frac{2}{N_o} \sum_{j=1}^m Q_1(t_j) \sqrt{2S} d_k + Q_2(t_j) \sqrt{S} d_k \cos \mathbf{q}_2 + I_2(t_j) \sqrt{S} d_k \sin \mathbf{q}_2 \right\} \quad (10)$$

where  $m$  is the number of L1 and L2 samples in one W-bit time, and  $A$  is a constant independent of the desired phase estimate  $\hat{\mathbf{q}}_2$  and the data polarity  $d_k$ .

Assume the W-bit data is statistically independent from bit to bit and has an equal probability of being +1 or -1, the above expression can be averaged over the probability density of the W-bit data to obtain:

$$P(Q_1, Q_2, I_2 | \mathbf{q}_2) = A \cosh \left\{ \frac{2}{N_o} \sum_{j=1}^m Q_1(t_j) \sqrt{2S} + Q_2(t_j) \sqrt{S} \cos \mathbf{q}_2 + I_2(t_j) \sqrt{S} \sin \mathbf{q}_2 \right\} \quad (11)$$

where cosh is the hyperbolic cosine function.

The Maximum A Posteriori estimator  $\hat{\mathbf{q}}_2$  of the L2 carrier phase can then be obtained by finding a local maximum of the joint probability function  $P(Q_1, Q_2, I_2 | \mathbf{q}_2)$  with respect to  $\mathbf{q}_2$ . Thus  $\hat{\mathbf{q}}_2$  must satisfy the following gradient equation:

$$0 = \frac{\partial}{\partial \mathbf{q}_2} P(Q_1, Q_2, I_2 | \mathbf{q}_2) \Big|_{\mathbf{q}_2 = \hat{\mathbf{q}}_2} = A \sinh \left\{ \frac{2}{N_o} \sum_{j=1}^m Q_1(t_j) \sqrt{2S} + Q_2(t_j) \sqrt{S} \cos \hat{\mathbf{q}}_2 + I_2(t_j) \sqrt{S} \sin \hat{\mathbf{q}}_2 \right\} \times \sum_{j=1}^m \left[ -Q_2(t_j) \sqrt{S} \sin \hat{\mathbf{q}}_2 + I_2(t_j) \sqrt{S} \cos \hat{\mathbf{q}}_2 \right] \quad (12)$$

where sinh is the hyperbolic sine function. Equation (12) is equivalent to the following when the sampled data summations are expressed as integrations:

$$0 = A \sinh \left\{ \frac{2}{N_o} \int_{kT_w}^{(k+1)T_w} r_1(t) \sqrt{4S} p(t) \cos(\mathbf{w}_1 t + \hat{\mathbf{q}}_1) dt + \frac{2}{N_o} \int_{kT_w}^{(k+1)T_w} r_2(t) \sqrt{2S} p(t) \cos(\mathbf{w}_2 t + \hat{\mathbf{q}}_2) dt \right\} \times \frac{2}{N_o} \int_{kT_w}^{(k+1)T_w} r_2(t) \sqrt{2S} p(t) \sin(\mathbf{w}_2 t + \hat{\mathbf{q}}_2) dt \quad (13)$$

where in (13)  $T_w$  is the W-bit time.

Instead of minimizing  $P(Q_1, Q_2, I_2 | \mathbf{q}_2)$  with respect to  $\mathbf{q}_2$  to find the MAP estimate of the L2 carrier phase, it is equivalent to perform the same on  $\ln\{P(Q_1, Q_2, I_2 | \mathbf{q}_2)\}$ , since the natural logarithm is a monotonic function. This results in the following gradient equation for  $\hat{\mathbf{q}}_2$ :

$$0 = A \tanh \left\{ \frac{2}{N_o} \int_{kT_w}^{(k+1)T_w} r_1(t) \sqrt{4S} p(t) \cos(\mathbf{w}_1 t + \hat{\mathbf{q}}_1) dt + \frac{2}{N_o} \int_{kT_w}^{(k+1)T_w} r_2(t) \sqrt{2S} p(t) \cos(\mathbf{w}_2 t + \hat{\mathbf{q}}_2) dt \right\} \times \frac{2}{N_o} \int_{kT_w}^{(k+1)T_w} r_2(t) \sqrt{2S} p(t) \sin(\mathbf{w}_2 t + \hat{\mathbf{q}}_2) dt \quad (14)$$

The closed loop structure that follows this equation is shown in figure 10.

As shown in figure 10, the L1-Y signal is first correlated with the locally generated L1 P-code, and then demodulated with a reconstructed local L1 carrier recovered from C/A code correlation, and integrated over one W-bit interval. Since the local L1 carrier is tracking the received signal, the I&D filter provides coherent matched filter detection of the L1 W-bit polarity on a bit-by-bit basis. A high W-bit error rate will be experienced, because the energy per W-bit is very low. However, the L1 W-bit I&D filter outputs, after correlating with L2, will still provide sufficient energy for L2 tracking with a narrow bandwidth phase-lock-loop. The I&D filter output is latched before cross-correlating with L2 since the L2 W-bit time is delayed by ionosphere with respect to L1.

Similarly, the L2 signal is first correlated with the locally generated L2 P-code in figure 10, and then demodulated into the inphase and quadrature components with a local estimate of the L2 carrier phase. Two I&D filters integrate the quadrature components over one W-bit interval.

Following equation (14) the loop error signal is generated as follows. The latched value of the L1 I&D filter output is weighted by the factor  $\sqrt{2}$  and added to the quadrature I&D output of the L2. The factor  $\sqrt{2}$  reflects the power difference between L1 and L2. The estimator favors the L1 W-bit estimate over the L2 W-bit estimate since L1 has a 3 dB power advantage. The hyperbolic tangent value of the sum of these two terms is multiplied with the L2 inphase channel to form the loop error signal, which is filtered by the loop filter. The loop filter output drives the VCO and achieves phase coherence by driving the loop error to zero, as demanded by the gradient equation.

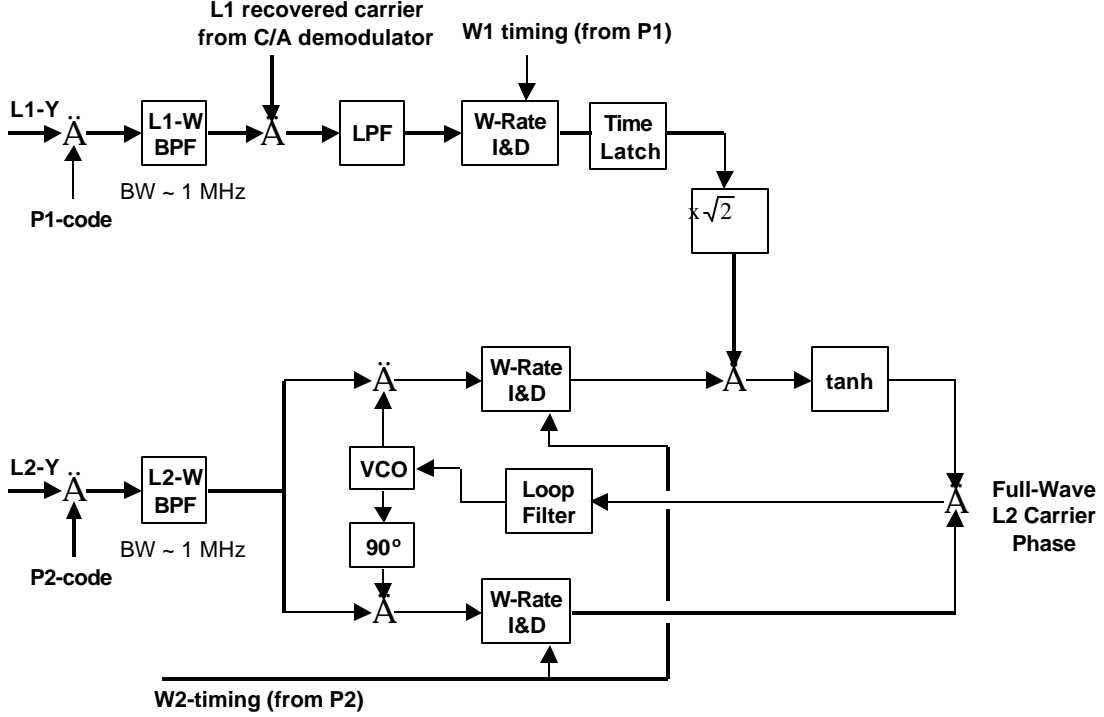


Figure 10. Semi-Codeless L2 Demodulation Structure Motivated by MAP

Without the L1 path the MAP structure in figure 10 is simply a L2 Costas loop with W-bit rate I&D arm filters. Since L1 and L2 have the same W-bit modulation, the MAP structure combines the L1 and L2 W-bit energies, and multiplies it with the L2 inphase channel to remove the unknown W-bit modulation. The hyperbolic tangent is the optimum nonlinearity over all carrier to noise density ranges. This can be demonstrated through computing the squaring loss of this loop.

### SQUARING LOSS OF THE MAP-MOTIVATED LOOP

From (14), the error signal that is to be driven to zero is seen to be the following, for the  $k^{\text{th}}$  W-bit period:

$$e_k = \tanh \left[ \frac{2}{N_o} (2Sd_k T_w + Sd_k T_w \cos \mathbf{f} + N_{1C} + N_{2C}) \right] \times \frac{2}{N_o} (Sd_k T_w \sin \mathbf{f} + N_{2S}) \quad (15)$$

where  $N_{1C}$ ,  $N_{2C}$ , and  $N_{2S}$  are the respective L1, L2 receiver noises integrated over one W-bit time by the I&D filters. They are independent, Gaussian random variables with means zero, and variances  $N_o T_w S$  for  $N_{1C}$ , and

$N_o T_w S/2$  for  $N_{2C}$  and  $N_{2S}$ . For simplicity, define the L2 W-bit energy per bit to noise density ratio to be  $R_d = S T_w / N_o$ , and the noise terms  $N_C = 2(N_{1C} + N_{2C}) / N_o$  and  $N_S = 2N_{2S} / N_o$ . Also,  $\phi$  is small during tracking. Then (15) can be written as:

$$e_k = \tanh(6R_d d_k + N_C) \times (2R_d d_k \sin \mathbf{f} + N_S) \quad (16)$$

The noise terms  $N_C$  and  $N_S$  are zero mean, independent Gaussian random variables with variances  $6R_d$  and  $2R_d$  respectively. The mean error signal is seen from (16), for small  $\phi$  to be:

$$\bar{e}_k = E[\tanh(6R_d d_k + N_C)] \times 2R_d d_k \mathbf{f} \quad (17)$$

where the expectation E is taken over the random noise term  $N_C$ . Since  $\tanh(x)$  is an odd function of x, the W-data modulation  $d_k$  is canceled in (17). The equivalent noise in the loop error signal is, from (16) and (17):

$$\mathbf{h}_k = \tanh(6R_d d_k + N_C) N_S \quad (18)$$

The noise  $\eta_k$  is zero mean. Its variance is given by

$$\text{var}(\mathbf{h}_k) = E[\tanh(6R_d d_k + N_C)]^2 \times 2R_d \quad (19)$$

The (one-sided) noise power spectral density of the

equivalent noise  $\eta_k$  around zero in frequency is given by

$$N_{eq} = 2 \text{var}(\mathbf{h}_k) T_W \quad (20)$$

Combining (17), (19) and (20) the SNR in the loop bandwidth  $B_L$  is obtained to be, after averaging over the random  $W$ -bit data:

$$\mathbf{r} = \frac{S}{N_o B_L} \times \frac{\{E[\tanh(6R_d + N_c)]\}^2}{E[\tanh(6R_d + N_c)]^2} \quad (21)$$

where in (21) the term  $S/N_o$  is used to designate the received carrier to noise density ratio on L2. Following the definition of  $S_L$  defined in (1), the squaring loss of the MAP motivated L2 loop is given by

$$S_L = \frac{\{E[\tanh(6R_d + N_c)]\}^2}{E[\tanh(6R_d + N_c)]^2} \quad (22)$$

The above has to be computed by performing numerical integrations for the mean and mean square expectations over the Gaussian density of  $N_c$ . The result is given in figure 12.

#### OPTIMALITY OF THE TANH NONLINEARITY

It is possible to show analytically that the hyperbolic tangent is the optimum nonlinearity that gives the minimum squaring loss. Following the same procedure as that leading up to (22), one can show that for any zero memory, odd nonlinearity  $G(x)$ , the squaring loss analogous to (22), is given by

$$S_L = \frac{\{E[G(6R_d + N_c)]\}^2}{E[G(6R_d + N_c)]^2} \quad (23)$$

Since  $N_c$  is Gaussian, zero mean, and with variance  $6R_d$ , the above is equivalent to

$$S_L = \frac{\left\{ \frac{1}{\sqrt{12pR_d}} \int_{-\infty}^{\infty} \exp\left[-\frac{(y-6R_d)^2}{12R_d}\right] G(y) dy \right\}^2}{\frac{1}{\sqrt{12pR_d}} \int_{-\infty}^{\infty} \exp\left[-\frac{(y-6R_d)^2}{12R_d}\right] G^2(y) dy} \quad (24)$$

Since  $G(x)$  is odd,  $G^2(x)$  is even. The integrals in (24) can be reduced to the following

$$S_L = \frac{\exp(-3R_d)}{\sqrt{3pR_d}} \times \frac{\left\{ \int_0^{\infty} \exp\left(-\frac{y^2}{12R_d}\right) \sinh(y) G(y) dy \right\}^2}{\int_0^{\infty} \exp\left(-\frac{y^2}{12R_d}\right) \cosh(y) G^2(y) dy} \quad (25)$$

Writing  $\sinh(x)$  as  $\cosh(x)\tanh(x)$ , and invoking the Schwartz's inequality

$$\left[ \int f(y)g(y)dy \right]^2 \leq \int f^2(y)dy \int g^2(y)dy \quad (26)$$

in which the equality sign holds only if  $f(y)$  and  $g(y)$  are proportional to each other, to the numerator of (25), and defining  $f(y)$  as  $G(y)[\cosh(y)\exp(-y^2/12R_d)]^{1/2}$ , and  $g(y)$  as  $\tanh(y) [\cosh(y)\exp(-y^2/12R_d)]^{1/2}$ , it can be shown that the numerator of (25) is upper bounded by

$$\leq \int_0^{\infty} G^2(y) \cosh(y) \exp\left(-\frac{y^2}{12R_d}\right) dy \times \int_0^{\infty} \tanh^2(y) \cosh(y) \exp\left(-\frac{y^2}{12R_d}\right) dy \quad (27)$$

with the upper bound reached only when the nonlinearity  $G(y)$  is proportional to  $\tanh(y)$ . Substituting (27) into the numerator of (25) the squaring loss for a general nonlinearity  $G(y)$  is found to be upper bounded by

$$S_L \leq \frac{\exp(-3R_d)}{\sqrt{3pR_d}} \int_0^{\infty} \tanh^2(y) \cosh(y) \exp\left(-\frac{y^2}{12R_d}\right) dy \quad (28)$$

The equality in (28) holds only when the nonlinearity  $G(y)$  is proportional to  $\tanh(y)$ . Since the largest  $S_L$  implies the smallest squaring loss, it is thus seen that the hyperbolic tangent does provide the minimum squaring loss among all zero memory, odd nonlinearities. Either (22) or (28) can be used to numerically compute the squaring loss of the MAP approach as a function of the L2 received  $C/N_o$ .

#### NEAR OPTIMUM L2 DEMODULATION MOTIVATED BY MAP

For low signal to noise ratio in the  $W$ -rate bandwidth, the following linear approximation for  $\tanh(x)$  is valid

$$\sinh(x) \cong \tanh(x) \cong x \quad \text{for small } x$$

With this approximation, the near-optimum structure for L2 phase tracking is the same as that shown in figure 10, with the only exception that the  $\tanh$  function is removed (i.e., replaced with its linear approximation). The squaring loss of this near-optimum approach can be computed from (23) directly by letting  $G(x)=x$ . It is easily computed to be

$$S_L = \frac{1}{1 + \frac{1}{6R_d}} = \frac{1}{1 + \frac{1}{6ST_w / N_o}} \quad (29)$$

Numerical values of (29) are shown in figure 12.

Before we compare the various approaches in terms of squaring loss, it is of interest to show that the MAP and near-MAP approaches do provide full wavelength L2 carrier recoveries. We will show this first with the near-MAP approach. Following figure 10, the signal component of the W-Bit rate I&D filter output in the L1 path is proportional, for the  $k^{\text{th}}$  W-Bit period, to  $\sqrt{2S}d_k$  where  $2S$  is the L1 received power. The inphase and quadrature W-Bit I&D filter outputs in the L2 path will have signal components  $\sqrt{S}d_k \sin \mathbf{f}$  and  $\sqrt{S}d_k \cos \mathbf{f}$ , respectively, where  $S$  is the received power of L2, and  $\phi$  is phase error in tracking L2. There is no phase error in the L1 I&D output since the L1 carrier phase is recovered from C/A code correlation. The 2-to-1-power relationship between L1 and L2 is preserved since the total power AGC's in both L1 and L2 receivers are noise loaded rather than signal loaded. This is typically the case in GPS and spread spectrum receivers. With the linear approximation of  $\tanh(x)$  the signal component in the loop error signal of the near optimal approach is then proportional to

$$\begin{aligned} & (\sqrt{2x}\sqrt{2S}d_k + \sqrt{S}d_k \cos \mathbf{f})x\sqrt{S}d_k \sin \mathbf{f} \\ & = 2S \sin \mathbf{f} + \frac{1}{2}S \sin 2\mathbf{f} \end{aligned} \quad (30)$$

As seen in (30) the loop error signal has a term proportional to  $\sin \phi$  and another proportional to  $\sin 2\phi$ . However, since the first term is weighted by a constant which is four times larger than that of the second, the error signal is dominated by the  $\sin \phi$  term, and full wavelength carrier phase can be reconstructed without half wavelength ambiguities. The S-Curve (i.e., loop error

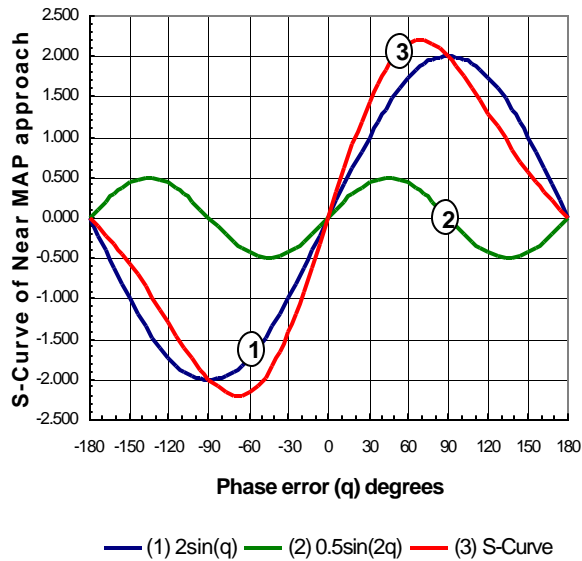


Figure 11. S-Curve of Near-MAP Approach

function vs. phase error), as expressed in (30), is shown in figure 11.

For the MAP approach with the  $\tanh(x)$  nonlinearity, the signal component in the loop error signal is proportional to

$$\begin{aligned} & \tanh(2\sqrt{S} + \sqrt{S} \cos \mathbf{f})x\sqrt{S} \sin \mathbf{f} \\ & \approx \tanh(\beta\sqrt{S})\sqrt{S} \sin \mathbf{f} \end{aligned} \quad (31)$$

Thus the MAP and the near MAP approaches will both provide full wavelength carrier phase recovery.

## PERFORMANCE COMPARISONS

The technique for recovery of L2 carrier phase measurements without knowledge of the Y-code should have two fundamental performance objectives. They should: (1) provide full-wavelength L2 carrier phase measurements without half wavelength ambiguities; and (2) minimize the squaring loss as much as possible.

Table 2 summarizes the squaring loss formulas developed for the various approaches discussed in this paper, and indicates whether full or half wavelength carrier phase measurement is available. The squaring technique has the largest squaring loss, and the MAP approach has the minimum squaring loss among all approaches.

The squaring loss for the various approaches are summarized in Table 1 for a number of L2 received  $C/N_0$ 's.

Table 1. Squaring Loss for various L2  $C/N_0$ 's.

Approach	27 dB-Hz	30 dB-Hz	33 dB-Hz	36 dB-Hz	39 dB-Hz	42 dB-Hz
Squaring	-43	-40	-37	-34	-31	-28
Cross-Correlation	-40	-37	-34	-31	-28	-25
P-code Aided Squaring	-30	-27	-24	-21	-18	-15
P-coded Aided Cross-Correlation	-27	-24	-21	-18	-15	-12
P-code aided L2 Costas	-27	-24	-21	-18	-15	-12
Z-Tracking	-26	-23	-20	-17	-14	-11
Soft-Decision Z-Tracking	-24	-21	-18	-15	-12	-9.5
Linear Approx. of MAP	-22	-19	-16	-13	-11	-8
MAP	-22	-19	-16	-13	-11	-8

APPROACH	Full or Half Wave-length	Squaring Loss for L2 demodulation
Squaring	half	$S_L \cong \frac{1}{1 + \frac{B_p}{2C/N_o}}$ $B_p \approx 20 \text{ MHz}$
Cross-correlation	full	$S_L \cong \frac{1}{1 + \frac{B_p}{4C/N_o}}$ $B_p \approx 20 \text{ MHz}$
P-code aided L2 squaring	half	$S_L \cong \frac{1}{1 + \frac{B_w}{2C/N_o}}$ $B_w \approx 1 \text{ MHz}$
P-code aided L2 Costas with W-bit I&D arm filters	half	$S_L \cong \frac{1}{1 + \frac{1}{2CT_w/N_o}}$ $T_w \approx 2 \text{ msec}$
P-code aided cross-correlation	full	$S_L \cong \frac{1}{1 + \frac{B_w}{4C/N_o}}$ $B_w \approx 1 \text{ MHz}$
Z-Tracking	full	$S_L = \text{erf}^2 \sqrt{2CT_w/N_o}$ $T_w \approx 2 \text{ msec}$
Soft Z-Tracking	full	$S_L \cong \frac{1}{1 + \frac{1}{4CT_w/N_o}}$ $T_w \approx 2 \text{ msec}$
Linear approximation of MAP	full	$S_L = \frac{1}{1 + \frac{1}{6CT_w/N_o}}$ $T_w \approx 2 \text{ msec}$
MAP	full	$S_L = \frac{\{E[\tanh(6R_d + N_c)]\}^2}{E[\tanh(6R_d + N_c)]^2}$ $N_c = \text{zero mean Gaussian, with variance } 6R_d$ $R_d = CT_w/N_o; T_w \approx 2 \text{ msec}$

**Table 2. Summary of Squaring Loss Formulas**

Figure 12 plots the squaring loss of the MAP, linear approximation of MAP, Soft-decision Z-Tracking, and Z-Tracking approaches, which are among the best in Table 2. Soft-decision Z-Tracking is about 2dB better than hard-decision Z-Tracking at 39 dB-Hz. The MAP approach performs about 3-dB better than hard-decision Z-Tracking at 39 dB-Hz since it applies soft-decision and utilizes the W-Bit energy in the L2 quadrature channel, in addition to the L1 quadrature channel, to cross-correlate with the L2 inphase channel. For  $C/N_o$  from 27 to 42 dB-Hz the linear approximation of MAP performs almost

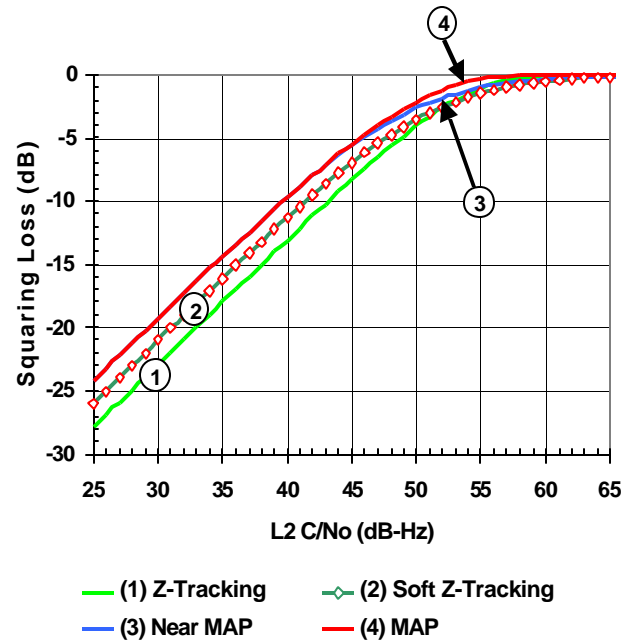


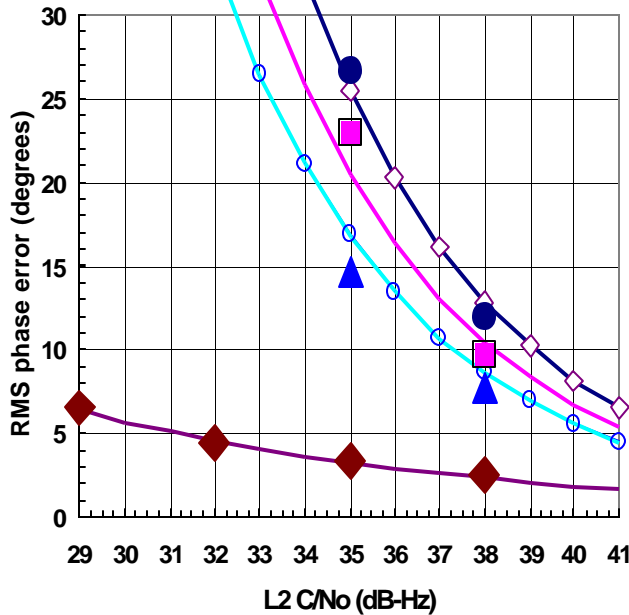
**Figure 12. Squaring Loss of MAP and its linear Approximation compared to Z- and Soft-Z**

identical to MAP (see Table 1). Only for  $C/N_o$ 's higher than 50 dB-Hz the MAP outperforms its linear approximation. Since the L2  $C/N_o$  is unlikely to be much higher than 45 dB-Hz, the linear approximation of MAP is equivalent to the MAP for all practical purposes.

Without knowledge of the Y-code the squaring loss for all approaches remains high in the realistic range of L2  $C/N_o$  achievable with a semi-spherical antenna which is required to receive GPS signals from a number of satellites. This is because the energy per W-bit over noise density ratio is very low (-15 dB at 39 dB-Hz), resulting in a high probability of error in the detection of W-Bit polarities (~40%).

The RMS phase errors for the MAP, near MAP, soft-decision Z-Tracking, and hard-decision Z-Tracking are compared to that of a phase-lock-loop with a loop bandwidth of 10 Hz in figure 13. The RMS phase error is computed using linear PLL theory, with equation (1). Also plotted in figure 13 are computer simulation results for the near MAP, soft-decision Z-Tracking, hard-decision Z-Tracking, and the ideal PLL. Computer simulation results agree with linear theory for relatively small RMS phase errors. As RMS error increases above 30 degrees computer simulation shows bigger RMS phase errors than linear theory, which is expected since the loop behavior becomes more nonlinear as RMS phase error becomes large and the linear theory is no longer accurate. Good agreement is however observed between linear theory and simulation for RMS phase errors < 30 degrees. Since the desired range of RMS error, for a good design,

is always less than 30 degrees, linear theory can be used effectively for all design purposes.



- ◆ Z-Tracking
- Linear approx. to MAP
- ◆ Linear PLL
- ▲ Linear approx. to MAP Simulation
- Z-Tracking Simulation
- ◆ Soft-decision Z-Tracking
- MAP
- ◆ Soft-Decision-Z Simulation

Figure 13. Computer simulation compared to linear PLL Theory, with Loop bandwidth=10 Hz.

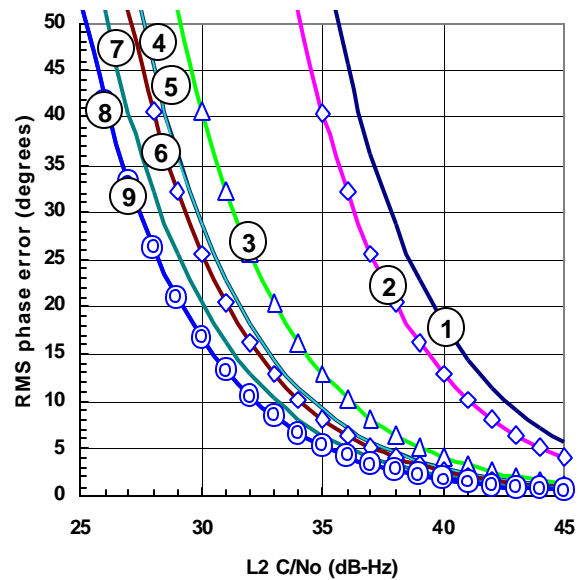
As shown in figure 13, even the MAP approach will require a L2 C/N<sub>0</sub> of 37 dB-Hz in order to maintain a RMS phase error of 10 degrees or less with the loop bandwidth of 10 Hz. This level of C/N<sub>0</sub> is not always available, especially for low elevation satellites.

However, a L2 loop bandwidth of 10 is often not necessary. L1 aiding is normally applied to L2 tracking in a GPS receiver to reduce the dynamics and oscillator instability faced by L2. This significantly reduces the requirement for a wide loop bandwidth. With L1 aiding, the L2 carrier loop bandwidth can be much smaller than 10 Hz. A typical loop bandwidth may be from 1 to 5 Hz, and is basically limited by truncation errors in the L1 aiding signal. Figure 14 shows the RMS phase error for all the approaches discussed in this paper for a loop bandwidth of 1 Hz. The results are computed using linear PLL theory with equation (1).

In actual surveying and RTK applications, cycle slip is a more serious concern than RMS phase error, even though large RMS phase errors, in fact, causes cycle slips. Unfortunately theory is not available for the mean slip time of a second order phase lock loop. Empirical and computer simulation data, however, are available in the literature [21-24]. The mean time to cycle slip is, in general, a function of the loop bandwidth B<sub>L</sub>, the RMS phase error σ<sub>φ</sub>, and the bias (steady-state) error φ<sub>ss</sub>. A numerical formulae obtained through curve fitting to the empirical and simulation data published in [21-24] is the following:

$$2B_L T_{slip} = 3.82 \exp\left[1.17 \times \frac{(1 - \sin f_{ss})}{4s_f^2}\right] \quad (32)$$

where T<sub>slip</sub> is the mean time between slips in seconds. Figure 15 shows the mean slip time for the 1 Hz loop bandwidth, and for all techniques discussed in this paper, assuming the bias error is zero.



- (1) squaring
- ◆ (2) cross-correlation
- ▲ (3) P-code Aided L2 Squaring
- (4) Code Aided Cross-correlation
- (5) P-code Aided L2 Costas with I&D filters
- ◆ (6) Z-tracking
- (7) Soft Z-tracking
- (8) Linear approx. to MAP
- (9) MAP

Figure 14. RMS phase error with 1 Hz loop bandwidth

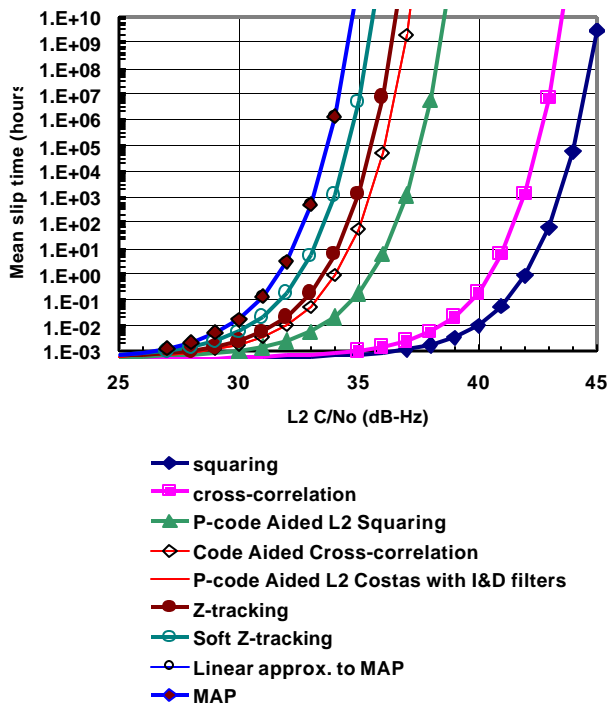


Figure 15. Mean cycle slip times ( $B_L=1$  Hz)

## SUMMARY AND CONCLUSION

Dual frequency L1 and L2 code and carrier phase measurements are important for carrier phase differential users to achieve their desired centimeter level of positioning accuracy in many applications such as surveying, machine control, and automatic construction. However, because of the encrypted Anti-Spoofing (AS) code on L2, unauthorized civilian users cannot recover the L2 carrier phase as easy as L1, which can be tracked after correlation with the C/A code. At least four techniques have been described in the literature previously to obtain the L2 carrier phase without knowledge of the W-bit polarities in the AS code: squaring, cross-correlation, P-code aided L2 squaring, and Z-Tracking. This paper describes five additional approaches. Three of these new approaches are modification of existing approaches, with performance improvements. They are Pcode aided cross-correlation, P-code aided L2 Costas with integrate and dump arm filters, and soft-decision Z-Tracking. In terms of squaring loss at the nominal L2 received  $C/N_0$  of 39 dB-Hz, the P-code aided cross-correlation approach is 13 dB better than the original cross-correlation technique. The P-code aided L2 Costas approach is 3 dB better than the existing P-code aided L2 squaring technique. And the soft-decision Z-Tracking approach is 2 dB better than the hard-decision Z-tracking technique. The other two approaches described in this paper are motivated by maximum a posteriori

(MAP) estimation theory. The first approach, called the MAP approach, follows the gradient equation of the MAP estimator exactly. The second approach, called the near-MAP approach, is a linear approximation of the MAP approach. In the MAP approach both the L1 and L2 W-Bit estimates are combined optimally to multiply with, after going through a hyperbolic tangent nonlinearity, the L2 inphase channel to derive the loop error signal. In the near-MAP approach a linear approximation is used to replace the hyperbolic tangent function. The MAP approach is shown to be the optimum among all approaches considered, and the hyperbolic tangent is shown to be the optimal nonlinearity. However, the near MAP approach is shown to perform just as well as the MAP approach in the realistic range of L2 received  $C/N_0$ 's. Computer simulation results verified theory. Both MAP and its linear approximation perform about 3 dB better than hard-decision Z-Tracking and 1 dB better than soft-decision Z-Tracking.

When L5 is available after 2010 the question of measuring L2 carrier phase without access to the classified Y-code will become moot. However, before this happens, civilian users will continue to use codeless or semi-codeless techniques to recover L2 carrier phase and meet their accuracy requirements. This paper describes these techniques in some detail. It is intended also to serve as a historical summary of some of the civilian's effort in obtaining the best accuracy from GPS, which is indeed impressive, even when they do not have access to the anti-spoofing Y-code.

## ACKNOWLEDGEMENT

Sincere thanks are acknowledged here to James D. Litton and Ron R. Hatch. Jim Litton suggested the MAP approach to the author, and has given much encouragement to the author during the course of this work. Ron Hatch supplied most of the material regarding the need for L2 carrier phase for surveying and carrier phase differential users, and helped write most of the Introduction section of this paper.

## REFERENCES

1. R.R. Hatch, "The Synergism of GPS Code and Carrier Measurements," *Proceedings of the Third International Geodetic Symposium on Satellite Doppler Positioning*, New Mexico State University, February, 1982.
2. Counselman C.C., Gourevitch, S.A., "Miniature Interferometer Terminals for Earth Surveying: Ambiguity and Multipath with the Global Positioning System," *IEEE Trans. In Geoscience and Remote Sensing*, Vol. GE-19, No.4, October 1981.



3. Remondi, B.W., "Performing Centimeter-Level Surveys in Seconds with GPS Carrier Phase: Initial Results," *NOAA Technical Memorandum NOS NGS-43*, National Information Center, Rockville, Maryland, 1985.
4. Mader, G., "Dynamic Positioning using GPS Carrier Phase Measurements," *Manuscripta Geodaetica*, 1986.
5. Hatch, R.R., "Instantaneous Ambiguity Resolution," *Proceedings of the KIS Symposium*, Banff, Canada, September 1990.
6. Frei, E., Beutler, G., "Rapid Static Positioning based on the Fast Ambiguity Resolution Approach FARA: Theory and First Results," *Manuscripta Geodaetica*, Vol.15, 1990.
7. Mader, G., "Ambiguity Function Techniques for GPS Phase Initialization and Kinematic Solutions," *Proceedings of the 2<sup>nd</sup> International Symposium on Precise Positioning with the Global Positioning System*, Ottawa, Canada, September, 1990.
8. Hatch, R.R., "Ambiguity Resolution while Moving - Experimental Results," *Proceedings of ION GPS-91*, The 4<sup>th</sup> International Technical Meeting of the Satellite Division of the Institute of Navigation, Albuquerque, New Mexico, September, 1991.
9. Remondi, B.W., "Kinematic GPS without static Initialization," *NOAA Technical Memorandum NOS NGS-55*, National Information Center, Rockville, Maryland, 1991.
10. Taniura, K., Fuse, K., Takahashi, S., "Instantaneous Dual Frequency Ambiguity Resolution," *Proceedings of the National Technical Meeting*, The Institute of Navigation, Long Beach, CA, January, 1998.
11. Ashjaee, J., Helkey, R.J., Lorenz, R.G., Sutherland, R.A., "Global Positioning System Receiver with Improved Radio Frequency and Digital Processing," U.S. Patent No. 4,928,106, May 1990.
12. MacDoran, P.F., Miller, R.B., Buennagel, L.A., Whitcomb, J.H., "Codeless System for Positioning with NAVSTAR-GPS," *Proceedings of the 1<sup>st</sup> International Symposium on Precise Positioning with the Global Positioning System*, Vol.1, Rockville, Maryland, 1985.
13. Keegan, R.G., "P-code Aided Global Positioning System Receiver," U.S. Patent No. 4,972,431, Nov. 1990.
14. Lorenz R.G., Helkey, R.J., Abadi, K.K., "Global Positioning System Receiver Digital Processing Technique," U.S. Patent No. 5,134,407, July 1992.
15. Simon, M.K., Lindsey, W.C., "Optimum Performance of Suppressed Carrier Receivers with Costas Loop Tracking," *IEEE Transactions on Communications*, Vol. COM-25, No.2, Feb. 1977.
16. Simon, M.K., "On the Calculation of Squaring Loss in Costas Loops with Arbitrary Arm Filters," *IEEE Transactions on Communications*, Vol. COM-26, No.1, Jan. 1978.
17. Holmes, J.K., "Coherent Spread Spectrum Systems," John Wiley and Sons, 1982.
18. Woo, K.T., Huth, G.K., Lindsey, W.C., Holmes, J.K., "False Lock Performance of Shuttle Costas Loop Receivers," *IEEE Transactions on Communications*, Vol. COM-26, No.11, Nov. 1978.
19. Litton, J.D., Russell, G., Woo, K.T., "Method and Apparatus for Digital Processing in a Global Positioning Receiver," U.S. Patent No.5,576,715, Nov. 1996.
20. Viterbi, A.J., "Convolutional Codes and Their Performance in Communication Systems," *IEEE Transaction on Communication Technology*, Vol. COM-19, No.5, Oct. 1971.
21. Viterbi, A.J., "Principle of Coherent Communication," McGraw-Hill, New York, 1966.
22. Palmer, L., Klein, S., "Phase Skipping in Phase Lock Loop Configurations That Track Biphase or Quadriphase Modulated Carriers," *IEEE Transaction on Communications*, Oct. 1972.
23. Shanneman, R., Rowbotham, J., "Unlock Characteristics of the Optimum Type II Phase Locked Loop," *IEEE Trans. On Aerospace and Navigation Electronics*, Vol. ANE-11, No.1, 1964.
24. Atwood, S., "Demodulator Cycle Slipping," *Motorola Technical Memorandum 3401-210-13*, February 1985.